Available online at www.sciencedirect.com
ScienceDirect
Journal of Molecular Catalysis A: Chemical 263 (2007) 259–265
JOURNAL OF MOLECULAR CATALYSIS A: CHEMICAL
www.elsevier.com/locate/molcata

Grafting of palladium nanoparticles onto mesoporous molecular sieve MCM-41: Heterogeneous catalysts for the formation of an *N*-substituted pyrrol

Jan Demel [a,b], Jiří Čejka [b], Snejana Bakardjieva [c], Petr Štěpnička [a,*]

[a] *Charles University, Faculty of Science, Department of Inorganic Chemistry, Hlavova 2030, 12840 Prague 2, Czech Republic*
[b] *J. Heyrovský Institute of Physical Chemistry, Academy of Sciences of the Czech Republic, Dolejškova 3, 18223 Prague 8, Czech Republic*
[c] *Institute of Inorganic Chemistry, Academy of Sciences of the Czech Republic, 25068 Řež near Prague, Czech Republic*

Received 18 July 2006; received in revised form 30 August 2006; accepted 31 August 2006
Available online 7 September 2006

Abstract

Palladium nanoparticles, obtained by thermochemical reduction of palladium(II) acetate in propylene carbonate or in tetrahydrofuran with added tetrabutylammonium acetate (Bu_4NOAc), were deposited onto mesoporous molecular sieve MCM-41 (spontaneously or after solvent change) to give novel supported metal catalysts, which were characterized by chemical analysis, powder X-ray diffraction, nitrogen adsorption-desorption isotherms and high-resolution transmission electron microscopy (HR TEM). The materials, together with 10% Pd/C reference were utilized as catalysts in the condensation reaction of 2-aminoethanol with *cis*-butene-1,4-diol to afford *N*-(2-hydroxyethyl)pyrrol. Both supported catalysts showed significantly higher conversions that Pd/C, the one prepared in the presence of Bu_4NOAc being the most active. Catalysts isolated after the reaction and used repeatedly showed lower activity than fresh ones. This apparently reflects partial metal leaching from the solid support and aggregation of the metal particles that were demonstrated by catalytic tests and HR TEM measurements, respectively.

Keywords: Palladium; Nanoparticles; MCM-41; Pyrrol; Catalysis; High-resolution TEM; Powder X-ray diffraction

1. Introduction

Palladium compounds play a key role in the synthetic organic chemistry, mainly owing to their ability to catalyze the formation of synthetically important C–C, C–N, C–O, and C–S bonds [1]. Recently, it was demonstrated that many of these reactions can be performed equally well with fine dispersions of the palladium metal [2]. As compared to their bulk counterparts, metallic nanoparticles offer large surface area, high numbers of corners and edges as well as a high surface tension. Together with the fact that no elaborate ancillary ligands (typically phosphines) are required, this makes them particularly attractive for catalytic utilization [3].

The first mesoporous molecular sieves with narrow pore size distribution were prepared at Mobil Research and Development Corporation in early 1990s [4], by using supramolecular surfactant assemblies (namely long-chain alkyl amines) as the structure-directing agents, which were subsequently removed by calcination or solvent extraction [5]. Materials thus prepared are typically amorphous solids showing ordering on a longer distance. Later, it was demonstrated that variation of the structure-assembling agent allows for obtaining materials with the pore size ranging from about 2 nm up to 30 nm and large surface areas, exceeding even 1000 $m^2\,g^{-1}$ [6].

Mesoporous molecular sieves were extensively utilized in the preparation of reusable, noble-metal catalysts. One of the most commonly employed approaches towards catalyst immobilization is the attachment of a ligand in a noble metal complex onto the sieve surface via covalent bonds [7]. The resulting, so-called hybrid catalysts usually exert higher selectivities than conventional heterogeneous catalysts. In addition, they can be easily separated from the reaction mixture and re-used. Unfortunately, the noble metal leaching from the support, which causes a decrease in the catalytic activity, often complicates recycling of these catalysts.

* Corresponding author. Fax: +420 221 951 253.
E-mail address: stepnic@natur.cuni.cz (P. Štěpnička).

1381-1169/$ – see front matter © 2006 Elsevier B.V. All rights reserved.
doi:10.1016/j.molcata.2006.08.094

A complementary method for the preparation of highly active supported catalysts is represented by impregnation of a support with an appropriate metal precursor that is subsequently transformed into a catalytically active form [6,8], sometimes nanosized metal species [9]. Grafting of pre-formed noble metal nanoparticles onto solid supports has been studied much less [3a]. Palladium nanoparticles can be prepared by electrochemical, photochemical [10] or sonochemical reduction of metal salts [11]. However, the method used most commonly is a simple chemical reduction. It is usually achieved by action of alcohols, sodium tetrahydridoborate or molecular hydrogen in the presence of stabilizing agents that prevent aggregation of the metal particles, which are typically polymers [12], dendrimers [13], surfactants [14] or just highly polar solvents (e.g., propylene carbonate) [15]. The presence of these protecting agents is essential for preserving catalytic activity of the nanoparticles, as the latter dramatically drops with growth (aggregation) of the metal particles.

In this work we report about preparation and characterization of MCM-41-supported, chemically generated palladium nanoparticles and present a comparative catalytic study on their utilization in the palladium-catalyzed reaction of 2-aminoethanol with *cis*-butene-1,4-diol to give *N*-(2-hydroxyethyl)pyrrol [16,17].

2. Results and discussion

2.1. Preparation and characterization of the catalysts

Palladium nanoparticles were prepared by thermochemical reduction of palladium(II) acetate in propylene carbonate which itself served as the particle stabilizing agent [15] (catalyst I) or in tetrahydrofuran in the presence of tetrabutylammonium acetate [14] (catalysts II–IV). The nanoparticle dispersions were then mixed with mesoporous molecular sieve MCM-41, so as to give catalysts with palladium loading 0.1 mmol g^{-1} (catalysts I and II), 0.05 mmol g^{-1} (catalyst III), and 0.2 mmol g^{-1} (catalyst IV). The nanoparticles stabilized with the ammonium salt adsorbed spontaneously onto the molecular sieve immediately after the addition of the molecular sieve. By contrast, an addition of MCM-41 to the nanoparticles generated in propylene carbonate left the metallic particles virtually intact even after stirring for more than 12 h at room temperature. The deposition was finally induced by addition of a less polar solvent (diethyl ether).

The supported catalysts were filtered, thoroughly washed with diethyl ether and dried shortly in the air. We have observed that the final drying has a dramatic effect on the catalytic activity. For instance, catalysts dried at 40 °C overnight exerted significantly lower conversions (about two times), than those dried only at room temperature for 1 h so as to not evaporate all the diethyl ether. Hence, the catalysts presented in this study were worked up by the latter method. We assume that the observed loss of catalytic activity results predominantly from destabilization of the metallic particles after removal of the polar solvate molecules. Increased stability of palladium nanoparticles in polar solvents is well established; however, the exact nature of the stabilization mechanism remains yet unknown [15a].

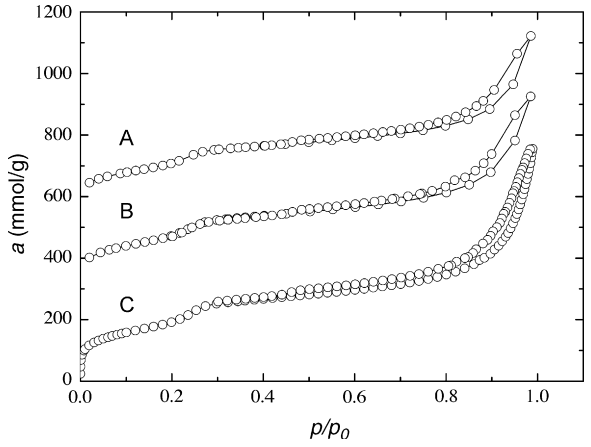

Fig. 1. Nitrogen adsorption isotherms of catalyst I (A), catalyst II (B) and MCM-41 (C). Isotherms for catalysts I and II are shifted by 300 and 550 mmol g^{-1}, respectively.

The supported catalysts were characterized by chemical analysis, powder X-ray diffraction, nitrogen adsorption isotherms and high-resolution transmission electron microscopy. It is noteworthy that the palladium loading calculated from the mass balance corresponded well with that determined by optical emission spectroscopy for mineralized samples, which points to a virtually complete reduction of the palladium precursor and deposition of the formed nanoparticles.

X-ray powder diffraction patterns observed for calcined mesoporous MCM-41 and catalysts I and II are very similar, showing three distinguishable peaks with $2\theta < 10^\circ$ that correspond with the ordered hexagonal framework of the parent MCM-41. This indicates that the structure of MCM-41 remains largely unaffected; a lower diffraction intensity of the Pd-MCM-41 materials as compared with their parent MCM-41 can be ascribed to a lower regularity of the catalysts as compared with the parent sieve.

Nitrogen adsorption isotherms recorded at −196 °C (Fig. 1) show characteristic increase in the adsorbed amount of nitrogen at about 0.3 (p/p_0) due to capillary condensation. Textural parameters, determined from the isotherms, indicate that the adsorption of the palladium nanoparticles causes a decrease in the surface area as well as the pore size (see Table 1).

2.2. Catalytic experiments

Catalytic activity of the newly prepared supported catalysts was assessed in the reaction of *cis*-butene-1,4-diol with

Table 1
Textural properties of MCM-41, catalysts I and II, and commercial 10% Pd/C

	S (m^2 g^{-1})	V_{meso} (cm^3 g^{-1})	d_{meso} (nm)
Catalyst I	539	0.169	2.9
Catalyst II	583	0.183	3.1
MCM-41	688	0.919	3.2
10% Pd/C	226	–	–

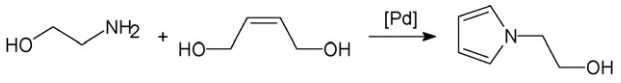

Scheme 1.

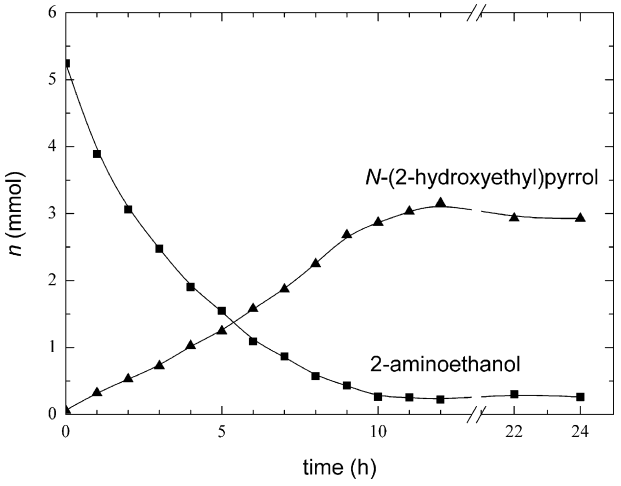

Fig. 2. Kinetic profile of the testing reaction with catalyst II at 120 °C: (■) 2-aminoethanol; (▲) *N*-(2-hydroxyethyl)pyrrol.

2-aminoethanol to give *N*-(2-hydroxyethyl)pyrrol (Scheme 1) [16]. The reaction was performed with ten-fold molar excess of *cis*-butene-1,4-diol with respect to the amine component in the presence of palladium in the supported form (catalysts I–IV), and with commercial Pd/C (10%) and MCM-41 for a comparison. The amount of palladium used in the catalytic reaction based on elemental analysis was 0.7 mol% (versus the aminoalcohol) for catalysts I and II, and 1 mol% for Pd/C for catalysts III and IV. The reaction was followed by gas chromatography using 1,2-bis[2-(methoxy)ethoxy]ethane as an internal standard. In all cases, *N*-(2-hydroxyethyl)pyrrol was the major product.

Kinetic profiles of the catalyzed reactions at 120 °C clearly showed the supported catalysts to have a higher activity than the commercial Pd/C, catalyst II being slightly more active than catalyst I (Figs. 2 and 3). In all cases, the pyrrol formation started practically immediately without a notable induction period. Increase in the reaction temperature to 140 °C resulted in a significant increase in the reaction rate; however, the product decomposed faster, too (Fig. 4). On the other hand, lowering of the reaction temperature to 100 °C had no beneficiary effect, as it led to a lowering of the reaction rate while not improving the reaction selectivity.

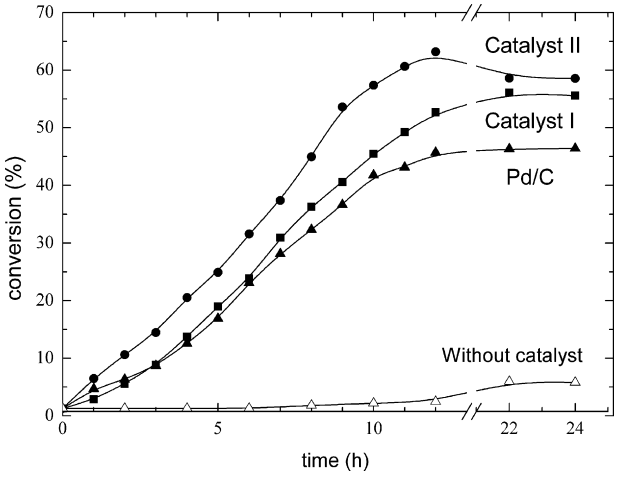

Fig. 3. A comparison of product formation at 120 °C in the presence of catalyst I (■), catalyst II (●), Pd/C (▲), and without added catalyst (△).

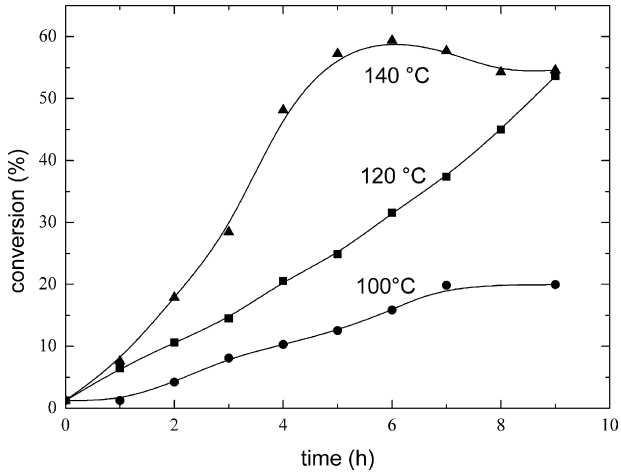

Fig. 4. A comparison of the rate of *N*-(2-hydroxyethyl)pyrrol formation in the presence of catalyst II at 140 °C (▲), 120 °C (■) and 100 °C (●).

In an attempt to study the influence of palladium loading, we have tested II-type (or Bu_4NOAc-supported) catalysts with different palladium content (0.5 and 2 mol%, catalysts III and IV) at similar Pd-to-substrate ratios. Rather surprisingly, both catalysts exerted conversions lower than catalyst II (Fig. 5). Finally, MCM-41 itself did not promote the condensation reaction at all.

We have also checked for heterogeneous nature of the catalyzed reactions by filtering the hot mixture after 4 h reaction time through 0.20 μm PTFE filter. The reaction proceeded even after removal of the catalyst, but with a rate four to five times slower. Very similar results were obtained when the reaction

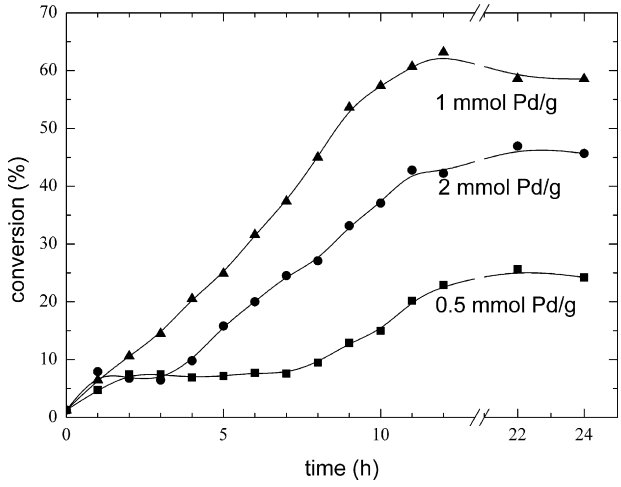

Fig. 5. A comparison of product formation in the reactions promoted by catalysts prepared with different palladium loading: catalyst IV (2 mmol g^{-1}, ●), catalyst II (1 mmol g^{-1}, ▲) and catalyst III (0.5 mmol g^{-1}, ■).

mixture was cooled to room temperature after 4 h of the reaction, filtered through the PTFE filter and the filtrate heated again to 120 °C. These observations indicate that palladium leaches from the support, which is, however, in keeping with the high polarity of the liquid reaction medium.

When the catalyst was recovered after the experiment, rinsed well with acetone and ethanol and used repeatedly, the catalytic activity dropped after two runs (Table 2). In order to check whether the decrease in the catalytic activity does not result from a deposition of (polymeric) organic products blocking the active species, we have performed similar recyclation tests with catalyst calcined before each repeated use (300 °C for 4 h). However, no significant difference between the catalysts re-used without and after calcination was observed. The lowering of the catalytic activity during the repeated use most likely reflects leaching of the metal from the support (see above), as well as aggregation of the palladium nanoparticles.

Table 2
Recyclation experiments with catalyst II, with and without calcination

Catalytic run without calcination	Yield (%)	Catalytic run with calcination	Yield (%)
1 (new catalyst)		55	
2	56	2	46
3	32	3	33
4	32	4	32

The latter assumption was corroborated by high-resolution transmission electron microscopy (HR TEM). We have performed qualitative rather than extensive observations and hence,

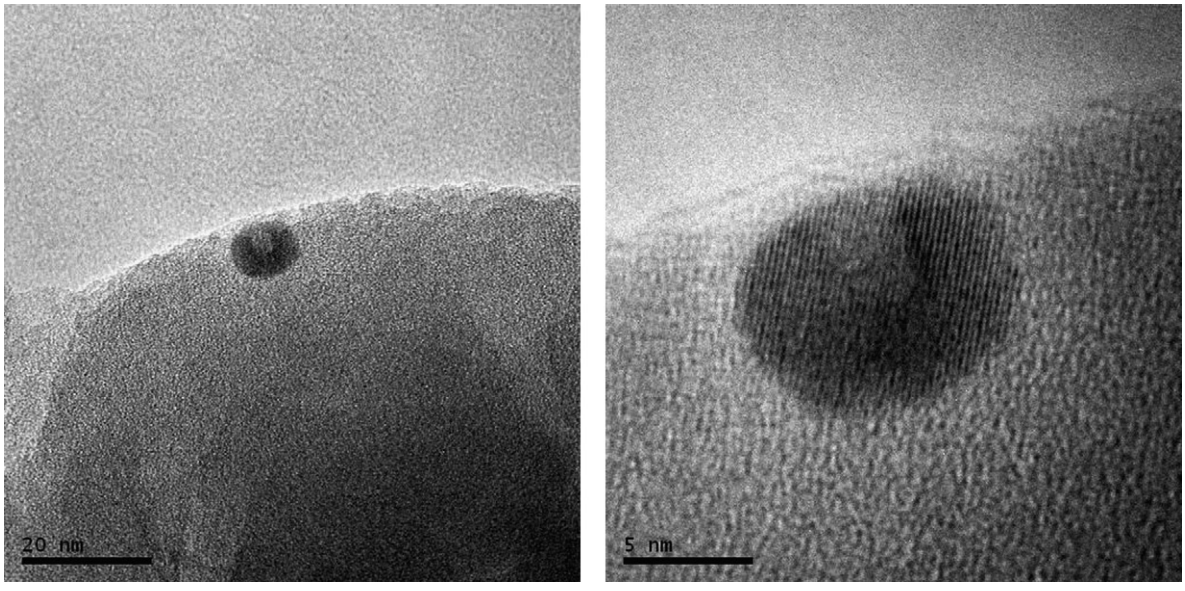

Fig. 6. HR TEM images of catalyst I showing an overall view (left) and a detailed snapshot of the metallic particle (right).

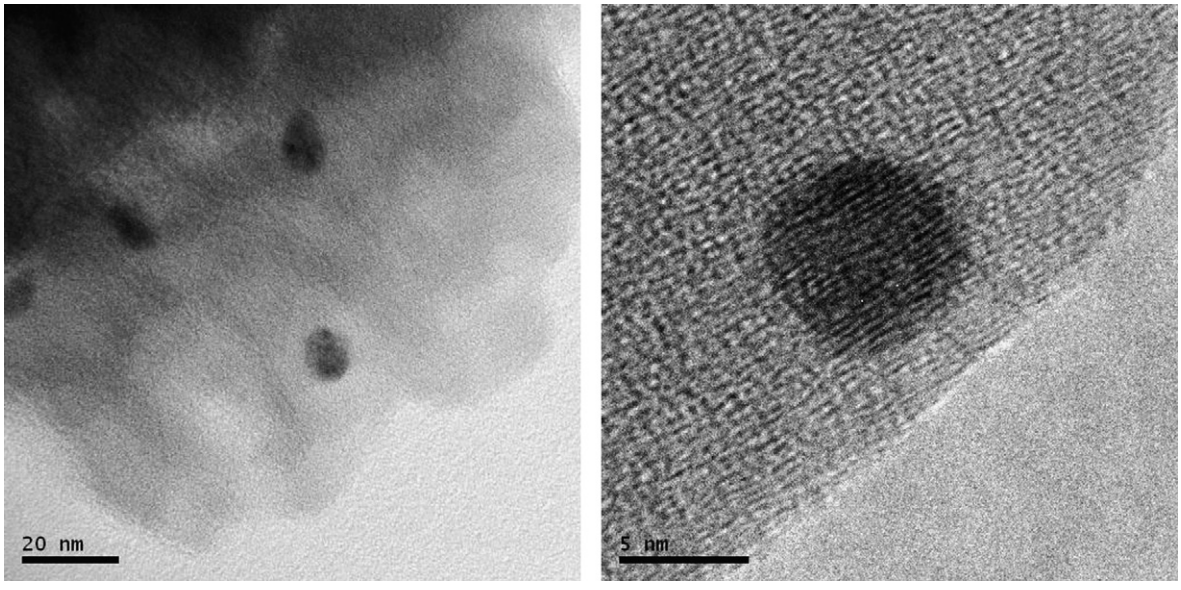

Fig. 7. HR TEM images of catalyst II: (left) an area accommodating several palladium nanoparticles and (right) a detailed view of a single metallic particle.

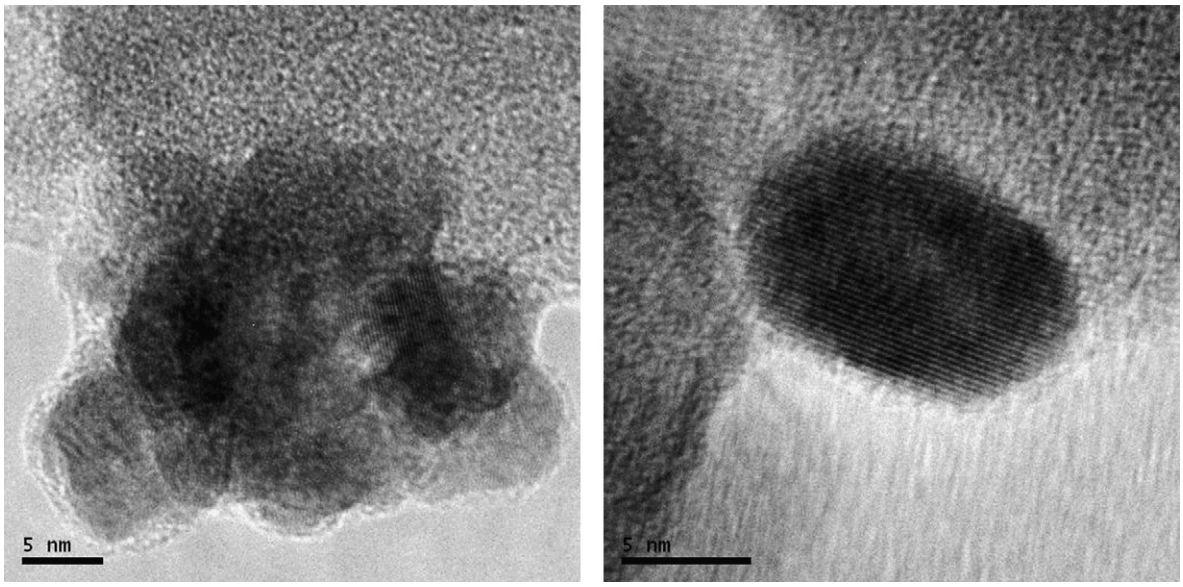

Fig. 8. HR TEM images of catalyst II after one catalytic run: views of an area accommodating an agglomerate (left) and a single particle (right).

do not present a statistical evaluation of the particle size. Nevertheless, the results of individual observations were consistent. HR TEM images obtained for the freshly prepared catalysts I and II revealed discrete spherical metallic particles with well-ordered internal structure, showing even interference from the lattice spacing (Figs. 6 and 7; particle diameters around 10 nm for catalyst I and around 7 nm for catalyst II). The interplanar distances determined from HR TEM images were 2.25 Å for catalyst I and 2.23 Å for both fresh and recovered catalyst II. These values correspond well with 2.25 Å (1 1 1) for face-centered cubic palladium [18]. More importantly, a comparison of HR TEM images recorded for fresh (Fig. 7) and used (Fig. 8) catalyst II showed that the metallic particles agglomerate during the reaction, while retaining their good crystalline structure. Another support came from powder X-ray diffraction measurements in the region of palladium 1 1 1 diffraction ($2\theta \approx 40^\circ$) [18]: Whereas the diffractogram recorded for unused catalyst II showed practically no peak, the same catalyst recovered after three runs (without calcination) displayed clearly discernible broad peak, which is in keeping with a larger diffraction volume of the aggregated particles (Fig. 9).

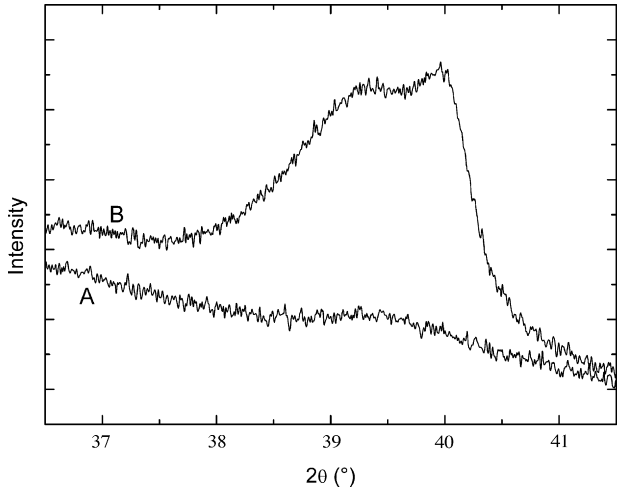

Fig. 9. X-ray diffractograms in the region of palladium 1 1 1 diffractions for catalyst II before (A) and three catalytic runs (B).

Apparently, the particle growth is not a simple process since the HR TEM images gave an evidence for both random aggregation of the spheric particles (see different orientations of the interference fringes in Fig. 8, left) and coherent growth of the individual metallic particles (Fig. 8, right). Nonetheles, in view of the observed leaching of the metallic particles from the support, the desorption/re-adsorption mechanism seems to be the plausible explanation of the particle aggregation process.

3. Summary

Palladium nanoparticles obtained from chemical reduction of palladium(II) acetate can be deposited onto mesoporous molecular sieve MCM-41 to afford supported materials that proved as active catalysts in the condensation reaction of 2-hydroxyethylamine with *cis*-butene-1,4-diol to give *N*-(2-hydroxyethyl)pyrrol. Metallic particles are leaching from the solid support during the catalyzed reaction. A lowered metal content together with aggregation of the metallic particles, which was confirmed by HR TEM and X-ray diffraction measurements, account for a decrease in the catalytic activity observed for recovered and repeatedly used catalysts.

4. Experimental

4.1. Materials and methods

All siliceous MCM-41 was prepared from sodium silicate (Riedel de Haen), hexadecyltrimethylammonium bromide (Fluka) and ethyl acetate (Fluka). The synthesis was carried out at 90 °C for 48 h and the template subsequently removed by calcination at 550 °C for 6 h (for details, see

[19]). Propylene carbonate (Aldrich), palladium(II) acetate (Aldrich), *cis*-butene-1,4-diol (Fluka), tetrabutylammonium acetate (Fluka), palladium over carbon (10%, Aldrich), and 1,2-bis[2-(methoxy)ethoxy]ethane (Fluka) were used without further purification. THF was distilled from potassium under argon. 2-Aminoethanol was distilled under vacuum and stored in sealed ampoules. All catalysts were handled in air.

Solution ^{1}H (399.95 MHz) and ^{13}C (100.58 MHz) NMR spectra were measured at 25 °C on Varian UNITY Inova 400 spectrometer. Chemical shifts (δ/ppm) are given relative to internal tetramethylsilane. X-ray powder diffractograms were recorded on a Bruker D8 X-ray powder diffractometer equipped with a graphite monochromator and position sensitive detector (Våntec-1) using Cu Kα radiation ($\lambda = 1.5412$ Å) in the Bragg–Brentano geometry arrangement. Nitrogen adsorption isotherms were measured with a Micrometritics ASAP 2020 volumetric instrument at −196 °C. The samples were degassed at 250 °C until presure of 10^{-3} Pa was attained (at least 24 h) prior to the sorption measurements.

Palladium content was determined on an ICP-OES spectrometer (IRIS Intrepid II; Thermo Electron Corp.) equipped with axial plasma and ultrasonic CETAC nebulizer, model U-5000AT+. The catalyst samples were first dried at 105 °C for several hours and then dissolved in a mixture of concentrated HF and HNO_3 (volume ratio 1/1; Suprapur, Merck) at 50 °C for 15 min and diluted with re-distilled water. Palladium was quantified using the 324.27 nm line, where the measured detection limit was 0.2 μg L^{-1}. The calibration was performed using blank (3% aq. HNO_3) and four standards covering the whole range of concentration measured. The standards were prepared by diluting a 1.000 g (Pd) L^{-1} standard solution (Analytika, certified solution).

High-resolution transmission electron micrographs were obtained on a Philips EM 201 instrument (80 kV). Copper grid coated with a holey carbon support film was used to prepare the samples: the catalyst samples were dispersed in little ethanol, sonicated for 10 min and the carbon coated copper grid was dipped into this suspension.

4.2. Grafting of palladium nanoparticles onto MCM-41

4.2.1. Preparation of catalyst I

Palladium(II) acetate (247 mg, 1.1 mmol) was dissolved in propylene carbonate (180 mL) and the solution was filtered through a Teflon syringe filter (0.45 μm pore diameter). The filtrate was heated at 110 °C for 3 h with stirring, whereupon the color of the reaction mixture slowly turned form orange to black as palladium nanoparticles formed. Then, MCM-41 (11.00 g) was introduced and the heterogeneous mixture was stirred at room temperature overnight. Diethyl ether (630 mL) was added to the mixture and stirring was continued for 30 min at room temperature. The resulting mixture was filtered on a glass frit and washed with diethyl ether (5 × 25 mL). The resulting grey powder was dried in air at room temperature for a short time so that all the diethyl ether was not evaporated.

Characterization: X-ray diffraction: 2θ (°) 2.45 (s), 3.95 (vw), 4.55 (w). Calculated from mass balance (complete reduction of palladium(II) acetate and adsorption of the formed palladium assumed): 1.05%. Elemental analysis of the bulk material: 0.5 and 0.6% Pd, which corresponds to 0.8 and 0.9% Pd in dry material.

4.2.2. Preparation of catalyst II

Palladium acetate (225 mg, 1.0 mmol) was dissolved in dry THF (150 mL) and the solution filtered through a Teflon syringe filter (pore size 0.45 μm). The filtrate was mixed with tetrabutylammonium acetate (945 mg, 3.15 mmol) and MCM-41 (10.00 g), and the mixture was refluxed for 4 h. During the refluxing period, the color of the mixture changed from orange to black. After the mixture was stirred overnight at room temperature, the resulting grey powder was filtered off and washed with diethyl ether (4 × 25 mL). The resulting powder was dried in air at room temperature for such a short time so that all the diethyl ether was not evaporated.

Characterization: powder X-ray diffraction: 2θ (°) 2.45 (s), 4.05 (vw), 4.65 (w). Calculated from mass balance (complete reduction of palladium(II) acetate and adsorption of the formed palladium assumed): 1.05% Pd. Elemental analysis: 0.7 and 0.8% Pd, which corresponds to 0.9 and 1.0% Pd in dry material.

4.2.3. Preparation of catalysts III and IV

Catalysts III and IV were prepared similarly as catalyst II, with Pd loading of 0.5 and 2 mmol g^{-1}, respectively.

Characterization of catalyst III. Elemental analysis: 0.4, 0.4% Pd (0.5, 0.5% Pd after drying). Calculated from mass balance (complete reduction of palladium(II) acetate and adsorption of the formed palladium assumed): 0.5% Pd.

Characterization of catalyst IV. Elemental analysis: 1.7, 1.8% Pd (2.6, 2.5% after drying). Calculated from mass balance (complete reduction of palladium(II) acetate and adsorption of the formed palladium assumed): 2.1% Pd.

4.3. Catalytic tests

Catalytic tests were performed in a three-necked flask (50 mL) equipped with a magnetic stirring bar, thermometer and a rubber septum, immersed in a thermostated oil bath (±2 °C). The reaction mixture consisting of 2-aminoethanol (285 mg, 5.0 mmol), *cis*-butene-1,4-diol (4.40 g, 50 mmol), 1,2-bis[2-(methoxy)ethoxy]ethane as an internal standard (265 mg, 1.5 mmol) was stirred and heated to the reaction temperature before the catalyst was introduced (in an amount corresponding to 0.05 mmol of palladium).

The progress of the reaction was monitored periodically on 0.1 mL aliquots (withdrawn via the septum by a syringe), which were diluted with acetone (0.1 mL) and centrifuged at 4000 rpm for 10 min. The samples were analyzed by a high-resolution gas chromatography (Agilent 6850 chromatograph equipped with a flame ionization detector and HB-1 column). The identity of the reaction product was checked by GC-MS (HP 5890 Series II, 5971A).

Recyclation experiments were performed at 120 °C for 12 h and only the final reaction mixture was analyzed. The solid catalyst was filtered off and thoroughly rinsed with ethanol and

acetone, and if appropriate, calcined in an air flow at 300 °C for 3 h (the temperature was increased by 1 °C min^{-1}). In one of the leaching tests, the solid catalyst was removed by filtration from hot reacting mixture after 4 h of reaction through a preheated frit and then a Teflon syringe filter (pore size 0.2 μm) while in the other, the reaction mixture was cooled to room temperature after 4 h, stirred for 2 h and then filtered through a sintered glass frit, and subsequently, a Teflon syringe filter (pore size 0.2 μm). The filtered reaction mixtures were then heated to 120 °C and periodically sampled as described above.

4.4. Isolation and characterization of N-(2-hydroxyethyl)pyrrol

A sample of *N*-(2-hydroxyethyl)pyrrol was isolated from the reaction mixture by diluting with water and extracting the resulting solution with diethyl ether (three times with 25 mL). The ethereal phase was dried over $MgSO_4$ overnight and the solvent was removed under reduced pressure. The oily residue was then distilled under vacuum on a Kugelrohr apparatus to give *N*-(2-hydroxyethyl)pyrrol as a colourless oil. The yield was not determined.

^{1}H NMR ($CDCl_3$): δ 3.85 (t, $^3J_{HH}$ = 5.2 Hz, 2H, CH_2OH), 4.03 (t, $^3J_{HH}$ = 5.2 Hz, 2H, NCH_2), 6.18 (t, $^3J_{HH}$ = 2.1 Hz, 2H, C*H*=CHN), 6.70 (t, $^3J_{HH}$ = 2.1 Hz, 2H, CH=*CH*N). ^{13}C{^{1}H} NMR ($CDCl_3$): δ 52.0 (s, *C*H_2OH), 62.8 (s, N*C*H_2), 108.5 (s, *C*H=CHN), 120.9 (s, CH=*C*HN). The NMR data are in agreement with the previously published results [16f].

Acknowledgements

This work was financially supported by the Czech Science Foundation (grant no. 104/05/0192) and is a part of the project "Center for Structure and Synthetic Application of Transition Metal Complexes" supported by the Ministry of Education, Youth and Sports of the Czech Republic (project no. LC06070).

References

[1] (a) A. de Meijere, F. Diederich (Eds.), Metal-Catalyzed Cross-Coupling Reactions, Wiley-VCH, Weinheim, 2004;
(b) E. Negishi, A. de Meijere (Eds.), Handbook of Organopalladium Chemistry for Organic Synthesis, vols. I–II, Wiley-Interscience, New York, 2002.
[2] (a) M. Beller, H. Fischer, K. Kühlein, C.-P. Reisinger, W.A. Herrmann, J. Organomet. Chem. 520 (1996) 257;
(b) Z. Novák, A. Szabo, J. Répási, A. Kotschy, J. Org. Chem. 68 (2003) 3327;
(c) H. Sakurai, T. Tsukuda, T. Hirao, J. Org. Chem. 67 (2002) 2721.
[3] (a) A. Roucoux, J. Schulz, H. Patin, Chem. Rev. 102 (2002) 3757;
(b) D. Astruc, F. Lu, J.R. Aranzaes, Angew. Chem. Int. Ed. 44 (2005) 7852;
(c) M. Studer, H.U. Blaser, C. Exner, Adv. Synth. Catal. 345 (2003) 45.
[4] C.T. Kresge, M.E. Leonowicz, J.W. Roth, J.C. Vartuli, J.S. Beck, Nature 359 (1992) 710.
[5] (a) F. Schüth, Chem. Mater. 13 (2001) 3184;
(b) J. Čejka, Appl. Catal. A 254 (2003) 327.
[6] For a review, see A. Corma, Chem. Rev. 97 (1997) 2373.
[7] D.E. De Vos, M. Dams, B.F. Sels, P.A. Jacobs, Chem. Rev. 102 (2002) 3615 (a review).
[8] (a) H. Bulut, L. Artok, S. Yilmazu, Tetrahedron Lett. 44 (2003) 289 (NaY zeolite);
(b) L. Artok, H. Bulut, Tetrahedron Lett. 45 (2004) 3881 (Y zeolite);
(c) K. Shimizu, T. Kan-no, T. Kodama, H. Hagiwara, Y. Kitayama, Tetrahedron Lett. 43 (2002) 5653 (sepiolite);
(d) A. Corma, H. García, A. Leyva, A. Primo, Appl. Catal. A: Gen. 257 (2004) 77 (sepiolite);
(e) A. Corma, H. García, A. Leyva, A. Primo, Appl. Catal. A: Gen. 247 (2003) 41 (K^+ and Cs^+ exchanged X zeolites);
(f) A. Corma, H. García, A. Leyva, Appl. Catal. A: Gen. 236 (2002) 179 (K^+ and Cs^+ exchanged Y and X zeolites).
[9] (a) I. Yuranov, P. Moeckli, E. Suvorova, P. Buffat, L. Kiwi-Minsker, A. Renken, J. Mol. Catal. A: Chem. 192 (2003) 239;
An in situ preparation of Pd nanoparticles from a phosphine-carbonyl Pd-complex has been described in:
(b) S. Behrens, G. Spittel, Dalton Trans. (2005) 868.
[10] G.A. Gaddy, E.P. Locke, M.E. Miller, R. Broughton, T.E. Albrecht-Schmitt, G. Mills, J. Phys. Chem. B 108 (2004) 17378.
[11] A. Nemamcha, J.L. Rehspringer, D. Khatmi, J. Phys. Chem. B 110 (2006) 383.
[12] (a) W. Wojtków, A.M. Trzeciak, R. Choukroun, J.L. Pellegatta, J. Mol. Catal. A 224 (2004) 81;
(b) R. Sablong, U. Schlotterbeck, D. Vogt, S. Mecking, Adv. Synth. Catal. 345 (2003) 333;
(c) C. Luo, Y. Zhang, Y. Wang, J. Mol. Catal. A: Chem. 229 (2005) 7;
(d) N. Semagina, E. Joannet, S. Parra, E. Sulman, A. Renken, L. Kiwi-Minsker, Appl. Catal. A: Gen. 280 (2005) 141;
(e) R. Narayanan, M.A. El-Sayed, J. Am. Chem. Soc. 125 (2003) 8340;
(f) A. Gniewek, A.M. Trzeciak, J.J. Ziołkowski, L. Kepiński, J. Wrzyszcz, W. Tylus, J. Catal. 229 (2005) 332.
[13] (a) R.M. Crooks, M. Zhao, L. Sun, V. Chechik, L.K. Yeung, Acc. Chem. Res. 34 (2001) 181, and references therein;
(b) Y. Jiang, Q. Gao, J. Am. Chem. Soc. 128 (2006) 716;
(c) Z.B. Shifrina, M.S. Rajadurai, N.V. Firsova, L.M. Bronstein, X. Huang, A.L. Rusanov, K. Muelen, Macromolecules 38 (2005) 9920.
[14] (a) M.T. Reetz, M. Maase, Adv. Mater. 11 (1999) 773;
(b) S. Mandal, A. Das, R. Srivastava, M. Sastry, Langmuir 21 (2005) 2408.
[15] (a) M.T. Reetz, J.G. de Vries, Chem. Commun. (2004) 1559;
(b) M.T. Reetz, G. Lohmer, Chem. Commun. (1996) 1921.
[16] S. Muharashi, T. Shimamura, I. Moritani, Chem. Commun. (1974) 931.
[17] This compound has been used as a synthetic precursor to local anesthetics (a) and in polymerizations (b–g):
(a) F.F. Blicke, E.S. Blake, J. Am. Chem. Soc. 53 (1931) 1015;
(b) G. Bidan, Tetrahedron Lett. 26 (1985) 735;
(c) M.G. Cross, D. Walton, N.J. Morse, R.J. Mortimer, D.R. Rosseinsky, D.J. Simmonds, J. Electroanal. Chem. 189 (1985) 389;
(d) G. Bidan, M. Guglielmi, Synth. Met. 15 (1986) 49;
(e) D. Stanke, M.L. Hallensleben, L. Toppare, Synth. Met. 55 (1993) 1108;
(f) D. Mecerreyes, J.A. Pomposo, M. Bengoetxea, H. Grande, Macromolecules 33 (2000) 5846;
(g) D. Mecerreyes, R. Stevens, C. Nguyen, J.A. Pomposo, M. Bengoetxea, H. Grande, Synth. Met. 126 (2002) 173.
[18] PDF card 5-0681: palladium, cubic, space group $Fm\bar{3}m$ (no. 225), a = 3.8898 Å at 26 °C; hkl 1 1 1, 2.246 Å, rel. int. 100, $2\theta \approx 40°$ at Cu Kα.
[19] J. Čejka, A. Krejčí, N. Žilková, J. Dědeček, J. Hanika, Microporous Mesoporous Mater. 44,45 (2001) 499.